Strong anisotrpoic maganetoresistance and magnetic interaction in La 0.7 Ce 0.3 Mn O 3 La 0.7 Ca 0.3 Mn O 3 p - n junction

H. Chou, Z. Y. Hong, S. J. Sun, J. Y. Juang, and W. J. Chang

Citation: Journal of Applied Physics **97**, 10A308 (2005); doi: 10.1063/1.1850378
View online: http://dx.doi.org/10.1063/1.1850378
View Table of Contents: http://scitation.aip.org/content/aip/journal/jap/97/10?ver=pdfcov
Published by the AIP Publishing

Strong anisotrpoic maganetoresistance and magnetic interaction in $La_{0.7}Ce_{0.3}MnO_3/La_{0.7}Ca_{0.3}MnO_3$ *p-n* junction

H. Chou[a] and Z. Y. Hong
Department of Physics and the Center for Nanoscience and Nanotechnology, National Sun Yat-Sen University, No. 70 Lian Hai Road, Kaohsiung, Taiwan, Republic of China

S. J. Sun
Department of Applied Physics, National University of Kaohsiung, Kaohsiung, Taiwan, Republic of China

J. Y. Juang and W. J. Chang
Institute and Department of Electrophysics, National Chiao-Tung University, ChinChu, Taiwan, Republic of China

(Presented on 9 November 2004; published online 28 April 2005)

The *p-n* junction made by colossal magnetoresistance materials, such as $La_{0.7}Ce_{0.3}MnO_3/La_{0.7}Ca_{0.3}MnO_3$, has great interest for its potential applications. However, the physics of the magnetic state and transport properties of the interface still remains open. In this article, bilayer $La_{0.7}Ce_{0.3}MnO_3/La_{0.7}Ca_{0.3}MnO_3$/STO films with a nearly perfect interface were studied. The *p-n* interface possibly becomes an antiferromagnetion-insulating layer as their parent compound, $LaMnO_3$, and confines the bias current flowing only on the top layer. The top and bottom layers interact with each other in a way that a strong anisotropy in magnetoresistance measurements was observed. © *2005 American Institute of Physics*. [DOI: 10.1063/1.1850378]

$La_{0.7}Ce_{0.3}MnO_3$ (LCeMO) and $La_{0.7}Ca_{0.3}MnO_3$ (LCaMO) are known as *n*- and *p*-type colossal magnetoresistance (CMR) materials with similar crystal structure and physical properties.[1–5] They experience the same paramagnetic-insulator–to–ferromagnetic-metal transition across the ferromagnetic-paramagnetic transition temperature (T_C) and metal-insulator transition temperature (T_P). Their parent compound $LaMnO_3$ with a pure Mn^{3+} configuration forms a canted antiferromagnetism (AFM) below 150 K.[6] When they are grown into a bilayer structure, a depletion layer due to carrier neutralization around the vicinity of the interface is expected. The potential application for a *p-n* junction by realizing rectifying function has been demonstrated elsewhere.[3–5] However, due to uncertain effects at the *p-n* interface, the incomplete depletion layer did not provide a perfect insulator layer as *p-n* junctions need. Excess insulator, such as a $SrTiO_3$ (STO) thin layer, was inserted to act as an artificial barrier for tunneling. Because the ferromagnetic property of CMR is mainly governed by the double exchange coupling mechanism,[7–9] the hopping of itinerant carriers across the interface is crucial. Though in a current perpendicular to the plane measurements of a *p-n* junction, an incomplete insulating characteristic[3,4] was observed, the magnetic state of the depletion layer and its interaction with the lateral ferromagnetic layers and the possible interaction between the lateral layers has not been studied systematically.

In this article, single LCeMO and LCaMO films and bilayer films were grown on $SrTiO_3$ (100) substrates by a pulse laser ablation system at 700–750 °C and P_{O2} = 300 mTorr. The thickness of films was calibrated to the number of pulses. The structure and compositional profile are analyzed by a x-ray diffractometer and by an Auger electrometer. The transport and magnetic properties were measured by a standard four points probe and by superconducting quantum interference device (SQUID) measurements.

Because of the lattice mismatch between the substrate and films, the strong tensile strain expands the in-plane lattice for films below a certain thickness.[1,10–14] To reduce the strain effect on the films that would suppresses the transition temperature of films, all single layers were grown up to a thickness of 100 nm. The bilayer films consisted of two 100 nm thick layers. According to the x-ray diffraction patterns as shown in Fig. 1, all films experience minor strain

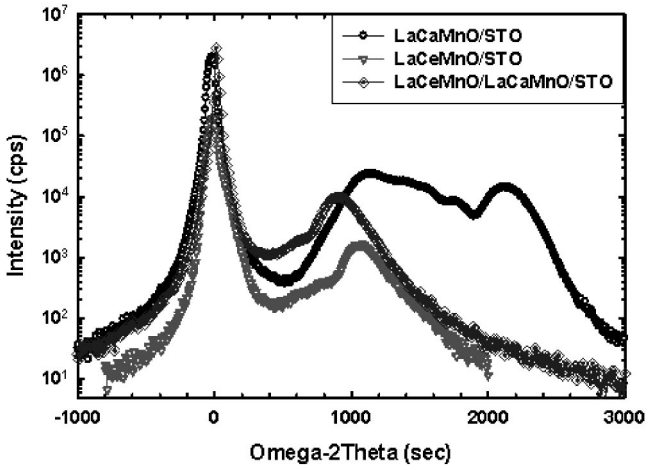

FIG. 1. The x-ray diffraction patterns, omega-2 theta scan, for the single-layer LCaMO film (black circles), the single-layer LCeMO film (black reverse triangles), and the bilayer films (the gray diamonds) around the (002) peak of $SrTiO_3$ (STO). The peaks of all films locate consistently around 1000 s on the right-hand side of STO (002) peak. This indicates a minor strain effect of the STO substrate on the films.

[a]Electronic mail: hchou@mail.nsysu.edu.tw

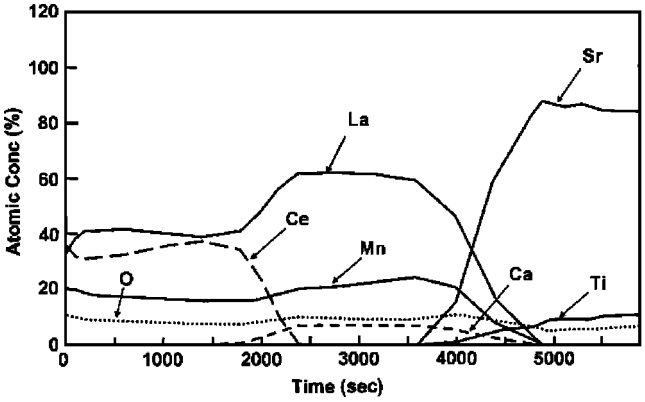

FIG. 2. The compositional profile of the bilayer film. The interface between LCeMO and LCaMO forms a clean interface with neither interdiffusion nor chemical reaction.

effect by the substrates, the (002) of LCaMO and LCeMO single layer films and the LCeMO/LCaMO bilayer film shift consistently only 1000 s from the (002) peak of STO. This implies a match in the lattice and a possible epitaxial growth of the bilayer film. Auger electrometer profile of the composition content of the bilayer film is shown in Fig. 2. A very clean interface with no traceable interdiffusion or reaction between LCeMO and LCaMO layers can be observed. Therefore, the possible interdiffusion or reaction suspected by C. Mitra *et al.*[3,4] can be neglected.

The current in-plane transport measurements for the resistance as a function of temperature were carried out at zero magnetic field and are shown in Fig. 3. The LCaMO film exhibits the highest metal-insulator transition temperature of 256 K with the lowest peak resistivity of 63 Ω cm. The single-phase LCeMO film can only be grown in a very narrow growth window and yields a lower transition temperature of 213 K with a medium peak resistivity of 133 Ω cm. The bilayer LCeMO/LCaMO film shows a medium transition temperature of 234 K and the largest peak resistivity of 365 Ω cm. The higher transition temperature of the bilayer film to the single layer LCeMO film could be because of the

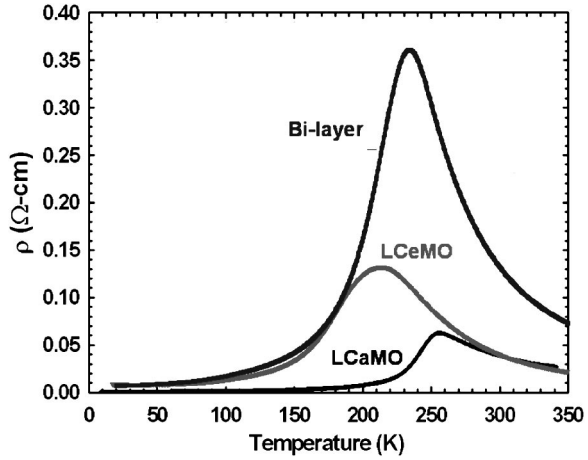

FIG. 3. The ρ-T characteristics measured at zero field condition. Due to the small growth window for LCeMO films and the large lattice mismatch with STO substrate, it exhibits lowest T_C. This mismatch was eased by growing LCeMO on the top of the LCaMO layer.

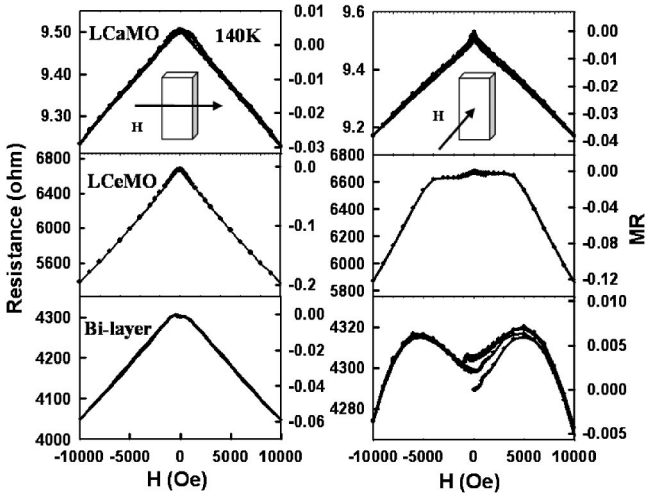

FIG. 4. The magnetoresistance of films as a function of applied field. All films show similar MR curves in the parallel configuration. In the vertical configuration, they have very different MR curves in the entire temperature range.

better lattice match between LCeMO on LCaMO than on STO. The total thickness of the bilayer equals the sum of each single layer, then the resistivity of the bilayer should be lower than any single film. However, the resistivity of the bilayer film moved in the opposite direction, indicating larger resistivity, which implies that the bilayer is separated by a high resistance interface layer. The current is then constrained to flow in the top layer with a reduced cross section or with a stronger spin fluctuation and yields a higher resistivity.

The magnetoresistance (MR) data for the parallel and vertical configurations and for the applied field parallel to or perpendicular to the substrate as shown in the diagram in Fig. 4, at 140 K indicates a strong anisotropic characteristic. In the parallel configuration, two single-layer films and the bilayer films have very similar MR response within 10 000 Oe. The LCeMO film shows the largest negative MR compared to the other films, which is believed due to the internal stress for single-phase LCeMO film on STO. In vertical configuration, the LCaMO film exhibits a similar MR curve. The smaller MR reading in the vertical configuration compared with the parallel configuration is due to the strong demagnetization effect of the ferromagnetic films. LCeMO film experiences a strong pinning at low field, which can be quenched for fields higher than 4500 Oe at 140 K. For the bilayer, an unexpected positive MR at low field is observed. The MR increases as field in both directions until a critical field of 6000 Oe is reached. Beyond the critical field, the diverse moments at the top layer start to align along the applied field and lower the MR to the negative region. The anisotropy could originate from the coupling between the top layer with the possible antiferromagnetism interlayer or with the bottom layer.

Though a SQUID can hardly sense the signal from the antiferromagnetic layer in between two ferromagnetic layers, the magnetic moment configuration of the top and bottom layers can be realized. In Fig. 5, the zero field cooled (ZFC) and field cooled (FC) magnetizations as a function of tem-

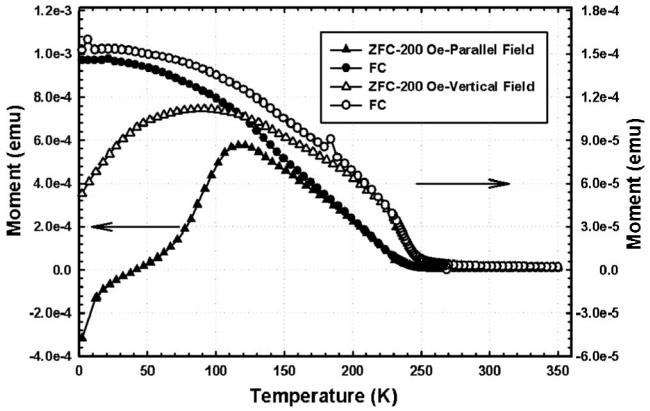

FIG. 5. The ZFC and FC magnetization curves of the bilayer film at 200 Oe in the parallel and vertical configuration. The small and negative ZFC magnetization and the huge difference between ZFC and FC magnetization at low temperature indicates a weak AFM coupling between the top and bottom layers and a strong anisotropy in the parallel and vertical configurations.

perature in both configurations are plotted. In parallel configuration, the ZFC curve at low temperature goes to negative due to the diamagnetic nature of the substrate. Compare with the FC curve at low temperature which is positive, 1×10^{-3} emu, the top and bottom layers form an antiferromagnetic (AFM) configuration along the direction parallel to the surface of the substrate. However, the AFM configuration can be easily quenched by a weak field of 200 Oe. In the vertical configuration, due to the demagnetization effect, the diamagnetic nature of the substrate is not strong enough to overcome the weak ferromagnetism in the direction perpendicular to the surface of substrate. The possible moment configuration of the system could be as shown in the Fig. 6. At low temperature, the top and bottom layers form an incomplete AFM configuration along the perpendicular direction and a nearly complete one in the parallel direction.

In this article we have grown bilayer films consisting of *n*- and *p*-type CMR layers with a very clean interface without noticeable interdiffusion or chemical reaction. The interface due to the carrier neutralization forms a high resistance depletion layer that confines the parallel current to flow on the top layer only. Because the parent compound of both types of compositions is a canted AFM insulator, the depletion layer has a high probability to yield similar properties as the parent compound. As a result of this, the lateral ferromagnetic layers forms weak AFM coupling via the depletion layer along the surface of films. The AFM coupling can be

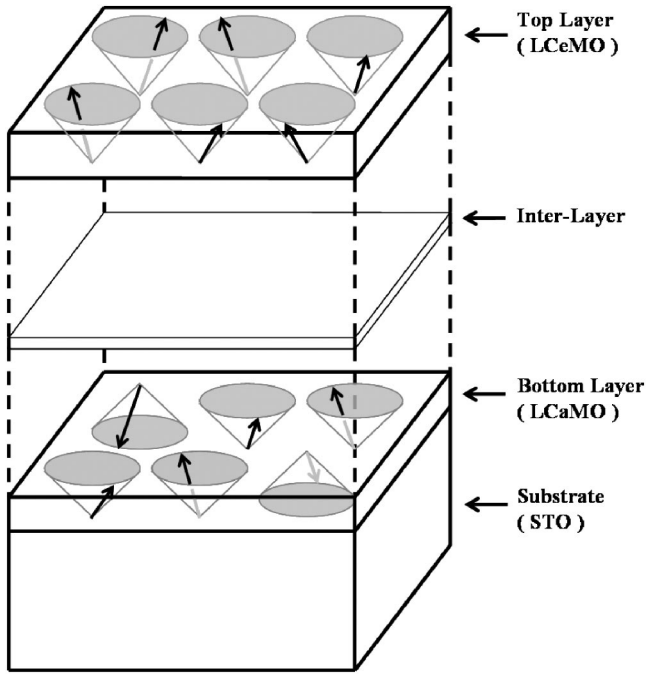

FIG. 6. The illustration of the possible magnetic state in the *p-n* bilayer. The magnetic coupling between the top and bottom layer is basically AFM at zero field along the direction of film surface, and yet forms a weak FM along the perpendicular direction.

quenched easily by a weak field of 200 Oe and produces the strong anisotropy in magnetic and electric transport measurements.

[1]S. Jin, T. H. Tiefel, M. McCormack, R. A. Fastnacht, R. Ramesh, and L. H. Chen, Science **264**, 413 (1994).
[2]J. M. D. Coey, M. Viret, and S. von Molnar, Adv. Phys. **48**, 167 (1999).
[3]C. Mitra, P. Raychaudhuri, G. Köbernik, K. Dörr, K.-H. Müller, L. Schultz, and R. Pinto, Appl. Phys. Lett. **79**, 2408 (2001).
[4]C. Mitra, P. Raychaudhuri, J. John, S. K. Dhar, A. K. Nigam, and R. Pinto, J. Appl. Phys. **89**, 524 (2001).
[5]P. Mandal and S. Das, Phys. Rev. B **56**, 15073 (1997).
[6]J. Zaanen, G. A. Sawatzky, and J. W. Allen, Phys. Rev. Lett. **55**, 418 (1985).
[7]C. Zener, Phys. Rev. **82**, 403 (1951).
[8]P. W. Anderson and H. Hasegawa, Phys. Rev. **100**, 675 (1955).
[9]P. G. de Gennes, Phys. Rev. **118**, 141 (1960).
[10]J. O'Donnell, M. S. Rzchowske, J. N. Eckstein, and I. Bozovic, Appl. Phys. Lett. **72**, 1775 (1998).
[11]S. Freisem, A. Brockhoff, D. G. de Groot, B. Dam, and J. Arats, J. Magn. Magn. Mater. **165**, 380 (1997).
[12]E. Gommert, H. Cerva, J. Wecker, and K. Samwer, J. Appl. Phys. **85**, 5417 (1999).
[13]F. Tsui, M. C. Smoak, T. K. Nath, and C. B. Eom, Appl. Phys. Lett. **76**, 2421 (2000).
[14]B. Vengalis, A. Maneikis, F. Anisimovas, R. Butkute, L. Dapkus, and A. Kindurys, J. Magn. Magn. Mater. **211**, 35 (2000).